Setting up a liquid crystal phase screen to simulate atmospheric turbulence

Michael K. Giles*[a], Anthony Seward[a], Mikhail A. Vorontsov[b], Jungtae Rha[a], Ray Jimenez[a]

[a]New Mexico State University, P. O. Box 30001, Dept. 3-O,
The Klipsch School of Electrical and Computer Engineering, Las Cruces, NM 88003

[b]Intelligent Optics Laboratory, U. S. Army Research Laboratory, Adelphi, MD

ABSTRACT

Phase screens are often used to simulate atmospheric turbulence in systems designed to test adaptive optics techniques. This paper presents the design and implementation of a dynamic phase screen using a simple and inexpensive twisted nematic liquid crystal display taken from a video projector and placed in a pupil plane. The details of the optical system layout, the system alignment procedure, and the operating parameters of the liquid crystal display are discussed. Examples of turbulence (having strength and statistics similar to measured values of atmospheric turbulence in a variety of scenarios) are written to the phase screen, and the effects of the turbulence on image quality are measured and presented.

Keywords: phase screen, atmospheric turbulence, simulation

1. INTRODUCTION

Applications of electrically addressed programmable nematic liquid crystal arrays, such as the active matrix liquid crystal displays used in video projectors, are not limited to standard display applications such as flat screen television monitors and projectors that require amplitude modulation. When operated in phase-mostly mode, a twisted nematic liquid crystal array becomes an optical phased array that can scan, align, collimate, focus, or shape a beam of light [1].

A phase-modulated liquid crystal array may be placed at any position in an optical system. When placed in a pupil plane and operated in phase mode, the liquid crystal display (LCD) becomes a programmable pupil function that can be used to generate any desired phase function. Since the nematic LCD is electrically addressable at rates on the order of 100 frames per second, its programmable pupil function can be dynamic. Thus, beam steering is accomplished by dynamically changing the frequency of a phase grating or by translating a phase Fresnel lens on the LCD. Beam alignment [2] is accomplished by detecting the position of the focused system point spread function at an image plane and then using the position information in a feedback loop to write an appropriate tilt or translation function on the LCD and move the focused spot to the desired alignment position. Autofocus is accomplished by closing a similar feedback loop that writes a Fresnel lens function of appropriate focal length on the LCD to maximize the encircled energy detected within a small region at the center of the focused spot.

Dynamic pupil functions written on a nematic LCD are especially useful in the field of adaptive optics. For example, an LCD placed in a pupil plane may be used to generate dynamic phase screens that simulate optical turbulence and enable a study of the effects of turbulence on the system image quality. A second LCD placed in another pupil plane may be used to generate an array of Hartmann lenslets to measure the wavefront function produced by the phase screen. A third LCD placed in still another pupil plane can be driven by the feedback signal from the Hartmann sensor to correct the distorted wavefront and improve the image quality [2].

* Correspondence: Email: migiles@nmsu.edu; WWW: http://www.ece.nmsu.edu/~optics/; Telephone: 505 646 DUDE; Fax: 505 646 1435

High-Resolution Wavefront Control: Methods, Devices, and Applications II,
John D. Gonglewski, Mikhail A. Vorontsov, Mark T. Gruneisen, Editors,
Proceedings of SPIE Vol. 4124 (2000) © 2000 SPIE. · 0277-786X/00/$15.00

A system comprising several phase-modulated LCDs, such as that described above, makes an excellent breadboard for testing new high-resolution adaptive optics techniques such as those that use adaptive interferometers. Recently, Seward, et al, introduced a new class of adaptive interferometers based on image plane masks that is well suited for many adaptive optics applications. This new class includes three adaptive interferometric implementations that use LCD-based image plane masks: the point diffraction, phase contrast, and dark ground interferometers [3]. The interferogram data produced by adaptive interferometers is used directly to close the feedback loop and drive the wave front-correcting LCD. In such a system, as in any adaptive interferometer, the fringes are erased as the wave front distortion is corrected [4, 5, 6].

The theory and algorithms used to calculate the appropriate phase patterns that should be written to a phase screen in order to simulate different conditions of atmospheric turbulence have been discussed previously by other authors [7, 8]. This paper does not address the issue of appropriate phase pattern generation, but rather, it describes the hardware implementation of an adaptive optics testbed that uses LCDs as phase screens to introduce and correct random wave front errors such as those produced by atmospheric turbulence. Section 2 describes the layout of the adaptive optics testbed. Sections 3 and 4 present the details of the characterization and alignment of the LCDs used as phase screens in the system. Finally, section 5 summarizes the results obtained using the LCD-based system.

2. LAYOUT OF THE HIGH-RESOLUTION ADAPTIVE OPTICS TESTBED

This section describes the implementation of a high-resolution adaptive optics testbed that uses three phase-modulated LCDs. The first LCD is used as a dynamic phase screen that simulates atmospheric turbulence, the second LCD is used as a wave front corrector, and the third LCD is used as a focal plane phase mask.

Fig. 1 is a schematic diagram of the testbed system. A helium neon laser beam enters the system at the bottom right, then passes through a microscope objective/pinhole spatial filter to form a point source whose light is collimated by the first lens. The collimated beam illuminates the first LCD which is used as a phase screen to simulate atmospheric turbulence. The first LCD is the system aperture stop. A two-lens 1:1 imaging system forms an image of the first LCD (a pupil plane) at the location of the second LCD which is used as the wavefront corrector. A second pupil plane is formed by subsequent lenses at the focal plane of the wave front sensor camera (left end of the third leg of the system near the top left corner of Fig. 1). The wave front sensor camera is used to visualize the spatially varying phase error introduced by the first LCD phase screen as well as the residual phase error after the wave front correction loop (left side of Fig. 1) is closed.

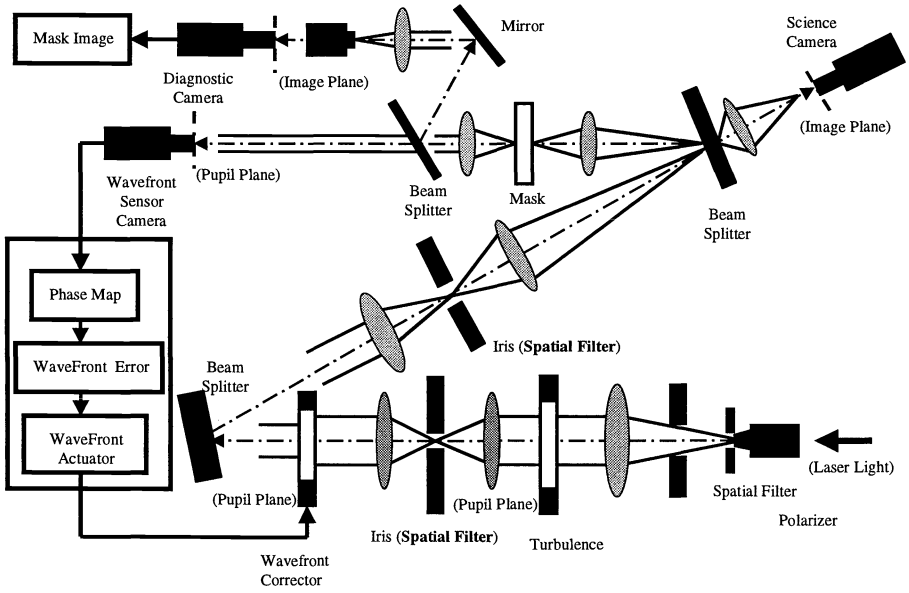

Figure 1. High-resolution adaptive optics testbed.

Five image planes (images of the point source) are formed by the system, two at the spatial filter locations, one at the science camera focal plane (upper right hand corner of Fig. 1), one at the mask, and one at the diagnostic camera focal plane (top of Fig. 1). The spatial filters, placed at the image planes between imaging lenses in both the bottom and middle legs of the system, filter the beam so as to remove the unwanted higher diffraction orders caused by the pixelated structure of the LCDs.

The science camera records the system point spread function (PSF) as the turbulence and wave front correction phase screens are changed and thus allows the changing PSF to be displayed in real time on a television monitor. The mask is a third LCD used as a focal plane mask to implement one of the three adaptive interferometers mentioned above. It is placed at an image plane as shown. The final image plane formed at the diagnostic camera is a magnified version of the focal plane mask that allows the structure of the mask to be seen superimposed on the system PSF in order to ensure that the PSF is adequately sampled by the pixelated LCD mask.

3. CHARACTERIZATION OF THE LCD PHASE SCREENS

Before the twisted nematic LCD can be used as a phase screen, its phase modulation characteristics must be measured. This section describes the method used to measure the phase modulation of the LCDs. The Dou double slit method [9], a technique that can be implemented in situ, is used for the phase measurements. The phase retardation is measured using the double slit interference principle. A linearly polarized collimated coherent light, polarized parallel to the director of the LCD, passes through the LCD, and a double slit is placed in front of the LCD as shown in Figure 2.

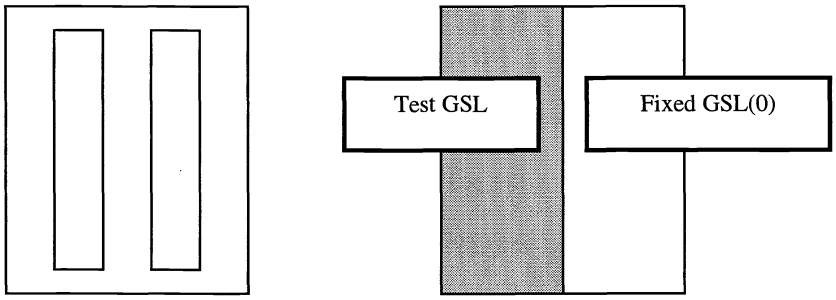

(a) Double slit (b) LCD

Figure 2. The set up for the Dou double slit technique.

The double slits are cut in an opaque film and are approximately 0.3 mm wide and 10 mm long with a 0.8-mm separation from center to center. In this experiment, a computer algorithm is used to write various gray scale levels (GSLs) to the LCD pixels behind one slit while the pixels behind the other slit have a fixed zero GSL as reference. This causes an optical path difference between the paths through the two slits because the voltage due to the GSL written to the LCD pixels changes the refractive index through one slit while the index (and optical path) through the other slit remains constant [9]. The detected fringes shift as shown in Figure 3 for vertical slits. The digitized point spread function of the vertical double slits is a horizontal sinc^2-modulated cosine fringe function as shown. The algorithm writes the rectangular box around the user-selected fringe-detection area and then tracks the fringe movement to measure the phase shift. Figure 3(a) shows the fringes (PSF) produced at the image plane by the double slits before any gray scales are written to the LCD. Fig. 3(b) shows the fringes shifted approximately 180 degrees when a test GSL of 100 is written to the pixels behind the test slit. Fig. 3(c) shows the fringes shifted approximately 360 degrees when a test GSL of 240 is written to the pixels behind the test slit.

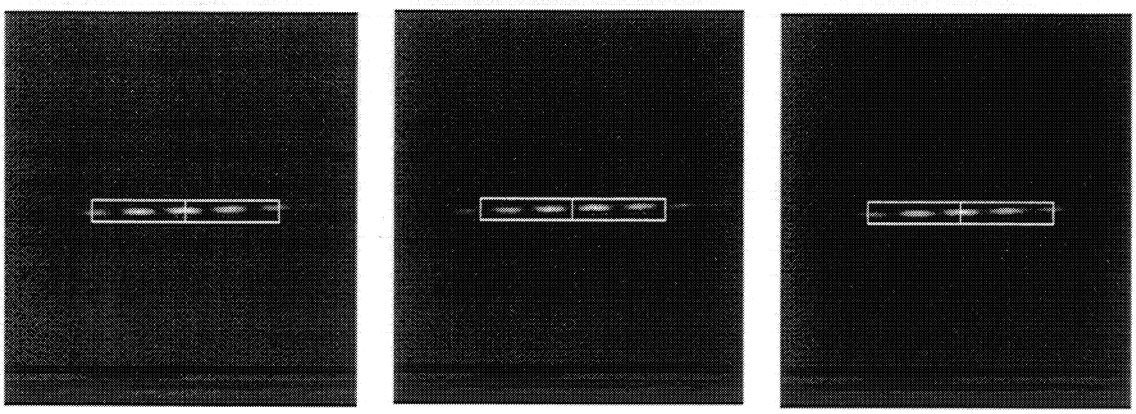

(a) GSL 0 (b) GSL 100 (c) GSL 240

Figure 3. Phase shift with varying GSL

The measured phase shift for a specific LCD is plotted as a function of GSL in Figure 4. It is nonlinear in the range from GSL 0 to GSL 240. This result plays an important role in the implementation of the turbulence and wave front corrector phase screens: the phase response curve for a given LCD must be incorporated in the algorithm that writes the phase function to that device in order to produce an accurate phase screen using that device.

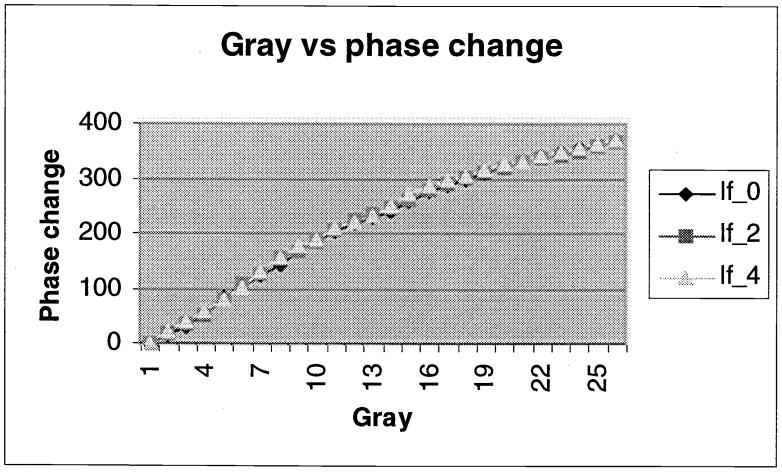

Figure 4. The phase response plot (phase change vs. GSL).

The amplitude modulation over the GSL range is also measured to determine its effect on the performance. Ideally, a phase screen will have no amplitude modulation. The optical setup to measure the amplitude modulation is shown in Figure 5.

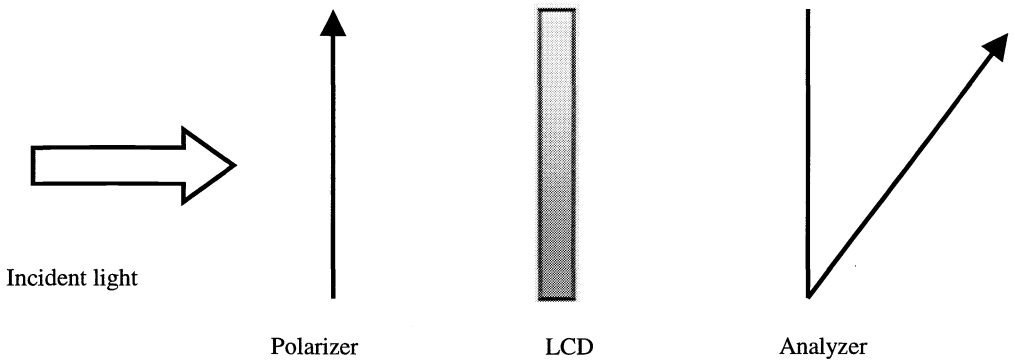

Figure 5. The scheme of the amplitude mode measurement

In order to measure the amplitude modulation, the LCD is placed between crossed polarizers. With zero voltage (GSL=0) across the device, the input polarization rotates through the twist angle. As the GSL on the LCD increases, the molecules tilt and the polarization does not rotate as much, so the output polarization angle changes. This causes the transmittance through the crossed polarizer (analyzer) to decrease. The result, plotted in Figure 6 for one specific device, shows that the transmittance is almost constant in the range $0 < GSL < 150$, but then it decreases in the range $150 < GSL < 250$. If the LCD is operated mostly in the GSL range of constant transmittance, it is possible to implement a phase screen with phase-mostly modulation and very little cross-coupled amplitude variation. This phase-mostly mode of operation depends on obtaining good alignment of the input polarization with the direction of the LCD molecules (director) of the LCD; however, misalignments of 2-4 degrees were acceptable for the phase screens tested in this experiment. Fig. 4 indicates very little difference in phase modulation for polarization/director misalignments of 0, 2, and 4 degrees.

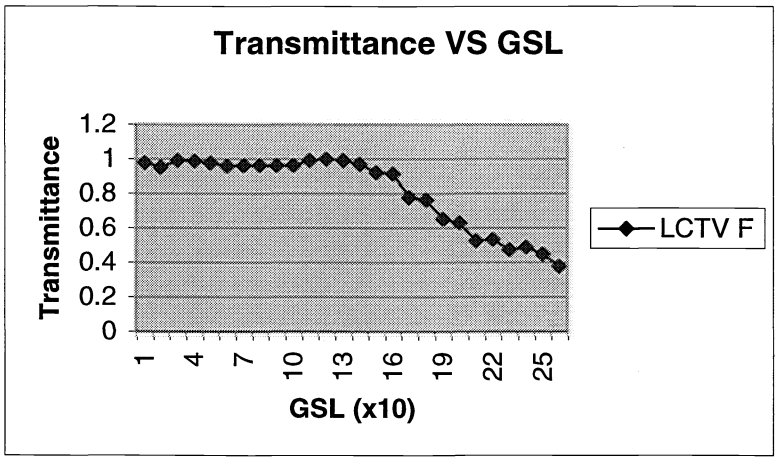

Fig. 6. LCD transmittance vs. GSL for phase-mostly operation.

4. ALIGNMENT TECHNIQUES

This section describes the critical alignment techniques used to set up a dynamic phase screen and phase corrector. As shown in Fig. 1, the turbulence phase screen and wave front corrector LCDs are placed in conjugate pupil planes by forming an exact image of the first LCD on the second LCD. Precise registration of the image of the first LCD on the second is an absolute requirement in order to operate this system effectively. Even a slight misalignment degrades the output image significantly. Precise registration is accomplished with a sequence of procedures. The most successful sequence utilizes the techniques in the following order with each successive method producing ever increasing alignment precision: (1) cross hair alignment, (2) ramp function alignment, and (3) frozen turbulence wave front conjugation. These techniques are discussed separately in the following paragraphs.

The most basic alignment technique involves the use of a cross hair routine that places a digitized cross hair image at the same location on each of the LCDs. The steps involved in using this technique are displayed sequentially in Fig. 7. Using the turbulence LCD as a reference, the position of the corrector device was adjusted using an X-Y micropositioning stage with micrometer adjustments. Fig. 7(a) shows the cross hair written on the turbulence phase screen, and Fig. 7(b) shows the two displaced cross hairs written on the two LCDs. The micrometer adjustments are moved slowly in each direction until the output image at the wave front sensor camera shows the superimposed cross hairs in Fig. 7(c). Each cross hair image is 2 pixels wide, so the precision of this result is approximately the pixel pitch which is 90 μm for these LCDs.

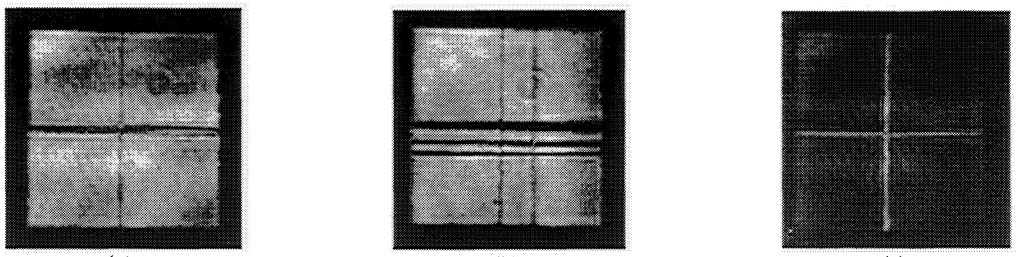

(a) (b) (c)

Figure 7. Cross hair alignment: (a) cross-hair on the reference LCD, (b) misalignment of the two LCDs, (c) best cross hair alignment.

The second method used in the alignment sequence involves a sampled ramp function written to each of the LCDs. When the maximum value of the gray level in each ramp is kept low, around 80, the ramp function works very well as an alignment tool. After the cross hair images are adjusted for the best perceivable alignment, the upper limit of the gray level is set and identical one-dimensional sampled ramp images are written to each LCD. This is done first in the x-direction (vertical gray scale bars), then in the y-direction (horizontal gray scale bars). In each case, even a slight misalignment is evident on the respective axis of the gray level bars as shown in figure 8(a) for a sampled ramp in the x-direction. The shadowed area seen at each gray level transition in Fig. 8(a) is representative of a slight misalignment. Fig. 8(b) shows the crisper gray level transition lines indicative of a better alignment. The precision of this method is approximately twice as good as that of the cross hair method, and it places the two LCDs in registration close enough that wave front correction is evident when one random phase function is placed on the first LCD and its conjugate on the other.

(a) (b)

Figure 8. Use of the ramp function alignment tool: (a) misalignment shown utilizing the ramp function, shown by spreading of the overlapping gray scale transition lines, (b) vertical alignment using the ramp function shown by crisp transitions between increasing gray scale levels.

Upon completion of the cross hair and gray scale ramp alignment steps, the final registration of the two LCDs is obtained by performing a true phase conjugation. This is done by placing a random phase pattern, representative of frozen atmospheric turbulence, on the first device, the exact conjugate phase pattern on the second, and then observing the resulting output system PSF. Fig. 9 is a gray scale representation of the frozen turbulence pattern, and Fig. 10 is the resulting degraded PSF caused when the turbulence pattern is placed on the turbulence phase screen.

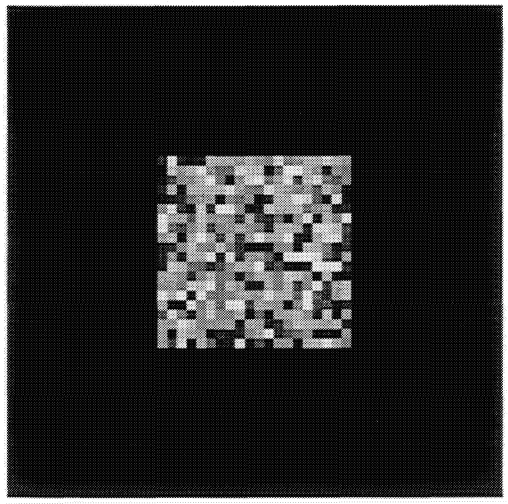

Figure 9. A random phase pattern written to the turbulence phase screen. Gray levels 0 to 255 represent phase values 0 to 2π.

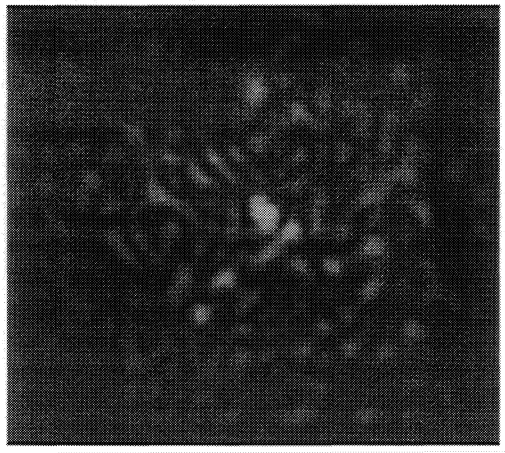

Figure 10. Degraded PSF produced by the turbulence phase screen.

The correction process is shown in Fig. 11. Fig. 11(a) shows the PSF before the random phase screen is placed on the turbulence phase screen. If perfect alignment has been achieved and if the second phase pattern is really the conjugate of the first when they are written to the devices, the placement of the conjugate phase screen on the corrector LCD will restore the PSF to a near perfect state. Since the initial alignment following steps (1) and (2) above is not perfect, the resulting PSF remains somewhat degraded. However, a slight movement of the X-Y micrometer adjustments soon produces the brightest possible PSF, and the alignment procedure is complete. Fig. 11(b) shows the resulting system PSF after the alignment process is completed. The resulting ratio of peak values of the two PSFs shown in Figs. 11(b) and 11(a) is 0.95, indicating very good correction and near perfect alignment.

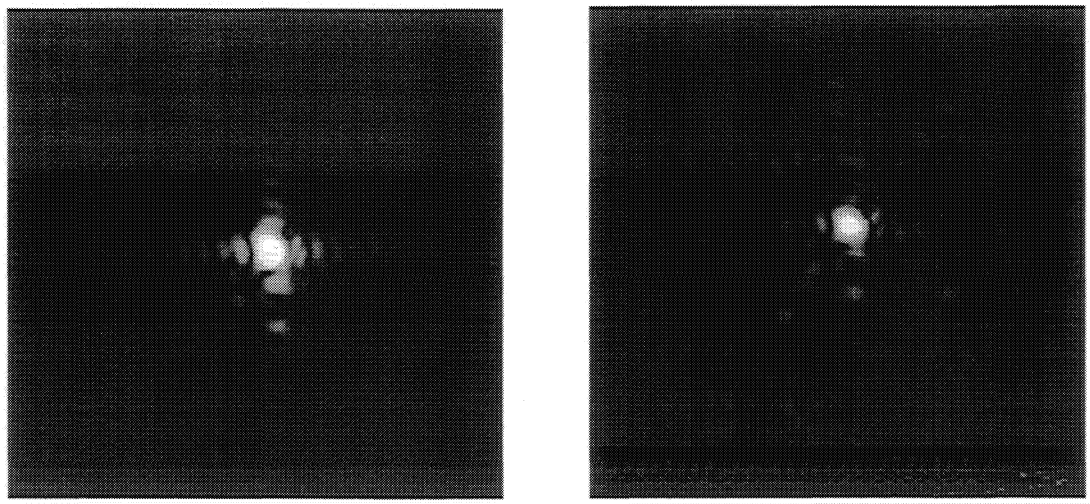

(a) (b)

Figure 11. System PSF (a) without any phase screen degradation, (b) after correction of the degraded PSF of Fig. 10.

5. CONCLUSIONS

The effective use of twisted nematic liquid crystal devices (LCDs) as dynamic phase screens has been demonstrated. An in situ technique has been developed to measure the phase response of each phase screen, and an effective alignment procedure for systems that utilize more than one phase screen has been developed. Finally, the use of LCD phase screens in a high-resolution adaptive optics testbed has been reported, and the use of phase screens in this testbed to simulate the effects of atmospheric turbulence has been shown.

ACKNOWLEDGMENTS

The authors acknowledge the support of the U. S. Air Force Office of Scientific Research for this work.

REFERENCES

1. M. K. Giles, "Applications of Programmable Spatial Light Modulators," invited paper for the *International Conference on Lasers 96*, Society of Optical and Quantum Electronics, 1996.

2. N. S. Prasad, S. Doyle, and M. K. Giles, "Collimation and beam alignment: testing and estimation using LCTVs," *Optical Engineering*, **35**, pp. 1815-1819, 1996.

3. A. Seward, F. Lacombe, and M. K. Giles, "Focal plane masks in adaptive optics systems," *SPIE Proceedings* **3762,** pp. 283-293, 1999.

4. R. Dou and M. K. Giles, "Closed-loop adaptive-ops system with a liquid-crystal television as a phase retarder," *Optics Letters* **20**, pp. 1583-1585, 1995.

5. R. Dou and M. K. Giles, "Phase measurement and compensation of a wavefront using a twisted nematic liquid crystal television," *Applied Optics* **35**, pp. 3647-3652, July 1996.

6. M. A. Vorontsov, R. Dou, G. Carhart, V. Sivokin, and M. K. Giles, "Iterative technique for high resolution phase distortion compensation in adaptive interferometers," *Optical Engineering* **36**, pp. 3327-3335, 1997.

7. D. A. Montera, B. L. Ellerbroek, and J. M. Brown II, "A phase and slope screen generator for spatially and temporally correlated unlimited length sequences," *SPIE Proceedings* **3353**, pp. 1070-1072, 1998.

8. R. G. Paxman, B. J. Then, and J. J. Miller, "Optimal simulation of volume turbulence with phase screens," *SPIEProceedings* **3763**, pp. 2-9, 1999.

9. R. Dou and M. K. Giles, "Simple technique for measuring the phase property of a twisted nematic liquid crystal television," *Optical Engineering* **35**, pp. 808-812, 1996.